

## **HALL EFFECT OF POLYPYRROLE-CHLOROPHYLL BLEND THIN FILM: A SOLAR CELL**

A.R.N. Laily<sup>1\*</sup>, M.I.N. Isa<sup>2</sup>, H. Salleh<sup>2</sup> and S. Hasiah<sup>2</sup>

<sup>1</sup>*Faculty of Electrical Engineering, Universiti Teknologi MARA (Terengganu)  
Sura Hujung 23000 Dungun, Terengganu, Malaysia*

<sup>2</sup>*Physical Sciences Department, Universiti Malaysia Terengganu, 21030 Kuala  
Terengganu, Terengganu, Malaysia*

*\*Corresponding author: norlaily77@tganu.uitm.edu.my*

### **ABSTRACT**

The blend of PPy with CHLO (PPy:CHLO) were prepared at 1:1, 1:5, 1:10, 5:1, and 10:1 ratios. The blend of PPy:CHLO thin films were deposited on Indium Tin Oxide (ITO) substrate (PPy:CHLO/ITO) by spin coating technique with different thicknesses. In this work, the Hall effect measurement (HEM) of PPy:CHLO/ITO thin film was investigated by HEM system in the square dimension of van der Pauw (vdP) geometry. From HEM study, the findings indicates that the samples were p-type of charge carrier, Hall voltage obtained only in mV which lies between  $1.17 \times 10^{-3}$  V to  $2.02 \times 10^{-3}$  V, Hall coefficient was  $1.17 \times 10^2$  cm<sup>2</sup>V<sup>-1</sup> s<sup>-1</sup> to  $2.0 \times 10^2$  cm<sup>2</sup>V<sup>-1</sup> s<sup>-1</sup>, the carrier concentration detected was between  $3.125 \times 10^{16}$  cm<sup>-2</sup> to  $5.330 \times 10^{16}$  cm<sup>-2</sup> and Hall mobility was between 33 cm<sup>2</sup>/Vs to 47 cm<sup>2</sup>/Vs. The results show that HEM of the samples was thickness dependence and this samples successfully investigated by Hall effect. These samples are suitable for electronic devices application.

*Keywords: Polypyrrole; Chlorophyll; blend thin film; Hall Effect;*

### **INTRODUCTION**

In recent years, conducting polymers have attracted much attention to chemists and physicists due to their versatile promising applications in many fields [1]. Among these conducting polymers, polypyrrole (PPy) has been one of the most studied polymers in the conducting polymer subject, since the monomer pyrrole is easily oxidized, water soluble and commercially available [2]. Pyrrole is capable of producing conducting polymers with high electrical conductivity, environmental stability and good redox properties. In addition, Chlorophyll (CHLO) is a natural dye made of magnesium salt complexes, hydrogenated in the 7,8-position, with a 6V-ethanone ring and chemically resembling haemin, an iron salt complex from mammalian blood [3]. It contains a porphyrin ring which in this study has been used as an organic material to investigate the electrical properties of PPy-CHLO blended as solar cell. A solar cell or photovoltaic cell is a device that converts solar energy into electricity by the photovoltaic effect.

Photovoltaic is the field of technology and research related to the application of solar cells as solar energy. Sometimes, the term solar cell is reserved for devices intended specifically to capture energy from sunlight, while the term photovoltaic cell is used when the source is unspecified [4]. The aim of the present study is to find out the Hall effect study of PPy-CHLO blended when the ratios of PPy-CHLO and the thickness were varied. Hall effect measurement has been used to determine more accurately the holes or electron concentration of the samples by minimizing the effect of the assumptions made when interpreting the concentration from the thermoelectric power measurements [5].

## EXPERIMENTAL METHOD

### *Samples Preparations*

The ITO substrates were cut into 1cm×1cm using micracuter 150 precision cutters (Nelson) and the diamond cutter. The cleaning process was done using ultrasonic vibrator (JEIOTECH model). The tank in ultrasonic vibrator was rinsed using distilled water to make sure it is cleaned [6]. 50ml beaker filled with distilled water and ITO substrates was put into the ultrasonic vibrator. Then, ITO substrates were thoroughly cleaned by distilled water, and the detergent. It was followed by acetone in order to remove any contaminations that might have been formed on the substrates [7] and distilled water, respectively. The time was set for 20 minutes, 30°C and mode vibration was set as medium for each cleaning. Lastly, the ITO substrates were dried using the dryer before kept into a Petri dish.

The preparation for PPy-CHLO solutions as follow; the concentration of PPy and CHLO was  $1.0 \times 10^{-4}$  M. The PPy-CHLO solutions were blended in volumetric flask with five different ratios as listed in Table 1.

Table 1: The volume of PPy and CHLO blended at different ratios

Ratios	Volume of PPy (ml)	Volume of CHLO (ml)
1:1	2.5	12.5
1:5	5.0	20.0
1:10	2.5	22.5
5:1	20.0	5.0
10:1	22.5	2.5

### *Thin Film Deposition Process*

Spin Coater Model WS-400B-6NPP-LITE was used. Spin coating is a procedure used to apply uniform thin films on the flat substrates. In short, an excess amount of the solvent is placed on the substrate, which is then rotated at high speed in order to spread the fluid by centrifugal force. In research by [8] stated that the higher the angular speed of spinning the thinner the film will be. The thickness of the film also depends on the

concentration of the solution.

In this work, PPy-CHLO blend thin films were deposited on ITO substrate using spin coating technique with different thicknesses. The thin film were varied with 0, 5, 10, 15, 20, 25, 30, 35, 40, 45, 50 layers. The spin coater used was 4 stages of spin; 500 rpm for 10 s, 1000 rpm for 15 s, 1500 rpm for 20 s and 2000 rpm for 30 s to complete one layer and then repeated to complete 5 layers, 10 layers until 50 layers for each samples. Figure 1 shows the thin film structure of thin film deposited on ITO substrates.

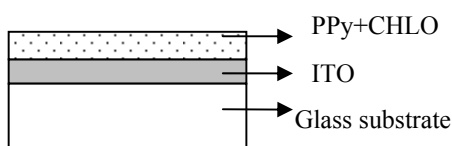


Figure 1: The structure of thin film

*Hall Effect Characteristics*

In HEM, the samples should have well-defined geometries and good ohmic contacts in order to obtain the accurate results. The samples must have vdP geometry. The ITO substrates were placed on the sample holder as shown in Figure 2. The sample on the holder system is then connected to contacts 1, 2, 3 and 4, using the silver paint on four edges. The connection to the contact is then tested using a multimeter.

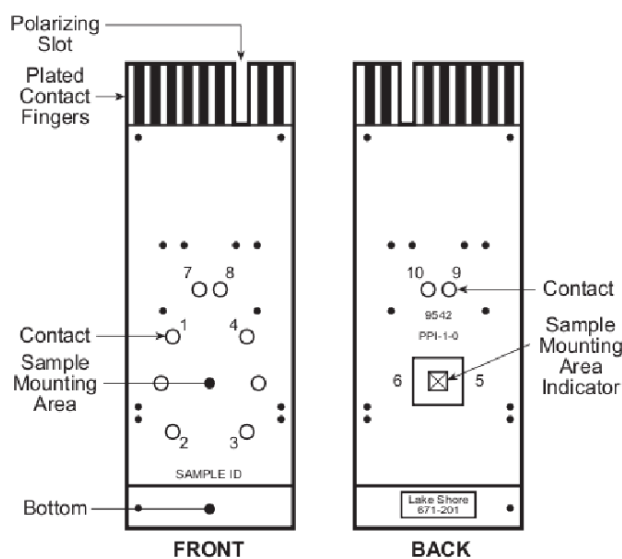


Figure 2: The geometry of sample holder [4]

The measurements were performed using the Leois-JSF software. The Hardware system called HEM system model 7600 is supplied by Lakeshore Ltd. The important part of this HEM system is ensuring that the room temperature and set temperature was equivalent (20 °C) in order to prevent the power supply from breakdown. The measurement consists of two parts. The first parts are called the IV curve traces

measurement and the second part is variable magnetic field measurement. The purpose of IV curve traces measurement is to make sure that all the contacts are in good connections. In this work, the magnetic field fixed was 10 kG (1 Tesla) and the current was 0.1 A.

In addition, Figure 3 shows the numbering of sample for Hall calculations which is used in this work.

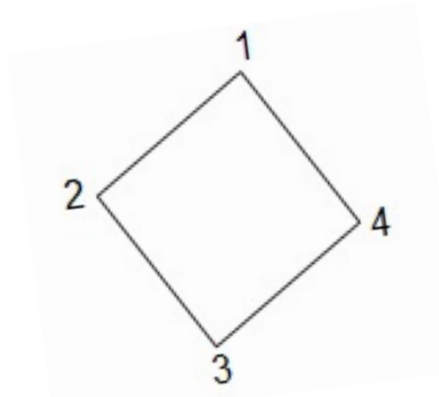


Figure 3: The numbering of sample for Hall calculations

Referring to Figure 3, the Hall voltage  $V_{+31,42 (+B)}$  is measured between contact point 4 and 2 when a current  $I_{+31}$  is passed from points 3 and 1. With field and current reversal, there will be eight voltages can be measured.

Hall voltage average,  $V_{H\text{ avg}}$ ;

$$= [V_{+31,42(+B)} - V_{+31,42(-B)} + V_{-31,42(-B)} - V_{-31,42(+B)} \dots - V_{+42,13(+B)} - V_{+42,13(-B)} + V_{-42,13(-B)} - V_{-42,13(+B)}] / 8 \quad (1)$$

The  $R_H$  in vertical ( $R_{HC}$ ) and horizontal ( $R_{HD}$ ) directions respectively are given as;

$$R_{HC} = 10^8 \frac{t[\text{cm}]}{B[\text{G}]}, \frac{V_{+31,42(+B)} - V_{-31,42(+B)} + V_{-31,42(-B)} - V_{+31,42(-B)}}{I_{+31(+B)} - I_{-31(+B)} + I_{-31(-B)} - I_{+31(-B)}} \quad (2)$$

And ;

$$R_{HD} = 10^8 \frac{t[\text{cm}]}{B[\text{G}]}, \frac{V_{+42,13(+B)} - V_{-42,13(+B)} + V_{-42,13(-B)} - V_{+42,13(-B)}}{I_{+42(+B)} - I_{-42(+B)} + I_{-42(-B)} - I_{+42(-B)}} \quad (3)$$

The Hall coefficient average,  $R_{H\text{ avg}}$  calculated by;

$$R_{H\text{ avg}} = \frac{R_{HC} + R_{HD}}{2} \text{ [cm}^2 \cdot \text{C}^{-1}\text{]} \quad (4)$$

The unit of  $R_H$  will be  $\text{m}^3\text{C}^{-1}$ , if  $t$  is in meter,  $B$  in Tesla, voltages in volt and current,  $I$  in ampere. If  $t$  is excluded, then  $R_H$  becomes the sheet Hall coefficient. When the thickness is unknown, the layer or sheet carrier concentration,  $n_s = n$ , is used instead of the bulk density,

$$n_s = \frac{8 \times 10^{-8} \times IB}{qV_H \text{ (total)}} \text{ cm}^{-2} \quad (5)$$

Where,  $B$  in Gauss unit,  $I$  in ampere, and  $V_H$  in volt. Then the Hall mobility ( $\mu_H$ ) is given by

$$\mu_H = \frac{|V_{H\text{ avg}}|}{\rho_{\text{ avg}}} \text{ [cm}^2 \cdot \text{V}^{-1} \cdot \text{s}^{-1}\text{]} \quad (6)$$

Lastly, types of charge carrier. It is determined by the polarity sign of  $V_{H\text{ avg}}$  from (1) and polarity sign of  $R_{H\text{ avg}}$  in (4). If the polarity sign is positive, the type of charge carrier is holes and called P-type. In contrast, if negative sign, it is electrons and called n-type. Equation (1) is [9] and (2-6) are [10].

## RESULTS AND DISCUSSION

In this work, varies PPy samples are referring to 1:1, 5:1, and 10:1 ratios samples while varies CHLO samples are subject to 1:1, 1:5 and 1:10 ratios samples. This ratios according to PPy:CHLO. In HEM, Hall voltage, Hall coefficient, carrier concentration, Hall mobility and types of charge carrier were determined.

### Hall Voltage

Figure 4 depicts the Hall voltage variation with the film thickness for the blended samples of varies PPy. The calculation was carried out using Equation (1).

Based on Figure 4 clearly shows that the Hall voltage is decreasing with the number of layers (thickness). This relationship agreed with the theory mentioned in Equation (7). The commercial ITO samples (at 0 layer of film), exhibited the highest Hall voltage 2.00 mV while the lowest Hall voltage detected for 1:1, 5:1 and 10:1 were 1.29 mV (at 40 layers), 1.25 mV (at 45 layers) and 1.17 mV (at 40 layers) respectively. The range of Hall voltage obtained for these varies PPy samples were between 1.17 mV to 2.00 mV. In addition, it is observed that as quantity of PPy increased in the blended samples of PPy:CHLO (which are 1:1, 5:1 and 10:1), the Hall voltage becomes smaller. This phenomenon could be attributed to the increase of charge concentration,  $n$  and the thickness,  $t$  as depict in equation below;

$$V_H = \left(\frac{1}{nq}\right) \left(\frac{IBz}{t}\right) \quad (7)$$

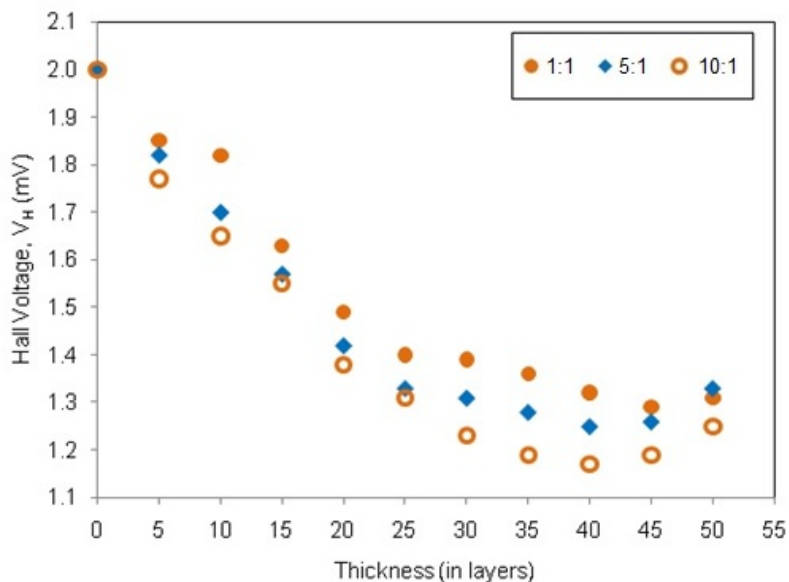


Figure 4: Hall voltage of varies PPy samples as a function of thickness

In contrast, Hall voltage raise as CHLO increased in the constant PPy samples as illustrated in Figure 5 which Hall voltage of varies CHLO samples versus the film thickness.

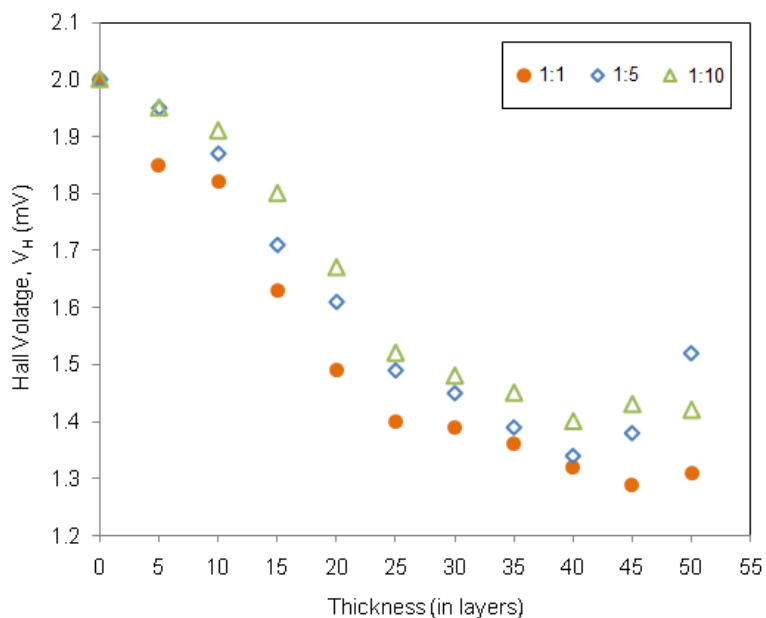


Figure 5: Hall voltage of varies CHLO with respect to the thickness

Figure 5, clearly shows that the Hall voltage for sample 1:1, 1:5 and 1:10 is decreasing with the number of layers (thickness). The range of Hall voltage obtained for these

varies CHLO samples were between 1.29 mV to 2.00 mV. The highest Hall voltage was 2.00 mV for the commercial ITO (0 layer of film) while the lowest Hall voltage obtained for sample 1:1 was 1.29 mV (at 45 layers), sample 1:5 was 1.34 mV (at 40 layers) and sample 1:10 was 1.40 mV (at 40 layers). From both graph, it is found that the Hall voltage of film clearly depend on the thickness and the quantity of materials used. In addition, the data also show that when the blended films thickness over 40, the Hall voltage increased. This trend can be explained as due to the decrease carrier concentration in the films. This is because the Hall voltage is reciprocal to the carrier concentration.

*Hall Coefficient*

Hall coefficient was characterized as shown in Figure 6 and Figure 7, against film thickness at room temperature and it was calculated from Equation (4). Figure 6 shows the Hall coefficient graph for varies PPy samples.

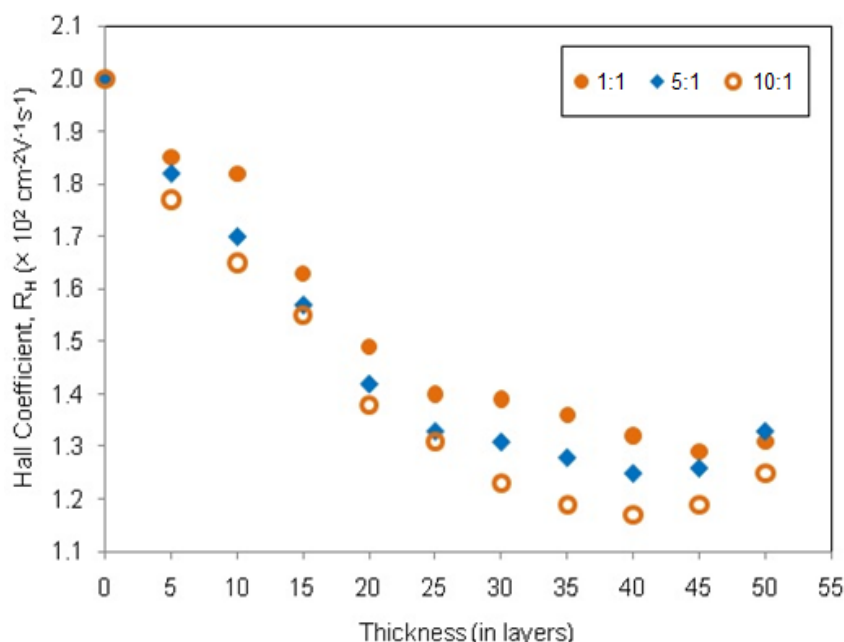


Figure 6: Hall coefficient against film thickness for varies PPy samples

The Hall coefficient dependence on film thickness was depicted in the Figure 6. The lowest Hall coefficient detected for sample of 0 layers with  $2.0 \times 10^2 \text{ cm}^2 \text{V}^{-1} \text{s}^{-1}$  while the lowest detected for sample 1:1, 5:1 and 10:1 was  $1.29 \times 10^2 \text{ cm}^2 \text{V}^{-1} \text{s}^{-1}$  (at 40 layers),  $1.25 \times 10^2 \text{ cm}^2 \text{V}^{-1} \text{s}^{-1}$  (at 45 layers) and  $1.17 \times 10^2 \text{ cm}^2 \text{V}^{-1} \text{s}^{-1}$  (at 40 layers) respectively. The range of Hall coefficient detected was between  $1.17 \times 10^2 \text{ cm}^2 \text{V}^{-1} \text{s}^{-1}$  to  $2.0 \times 10^2 \text{ cm}^2 \text{V}^{-1} \text{s}^{-1}$ . From these plots, it is apparent that the 1:1 film exhibited the highest Hall coefficient of varies PPy samples with respect to the film thickness. This is due to the amount of CHLO and PPy is balance for 1:1 sample compared to 1:5 and 1:10 which contained more CHLO. Hall coefficient decreased when thin film increased. The Hall coefficient for varies CHLO samples was presented in Figure 7.

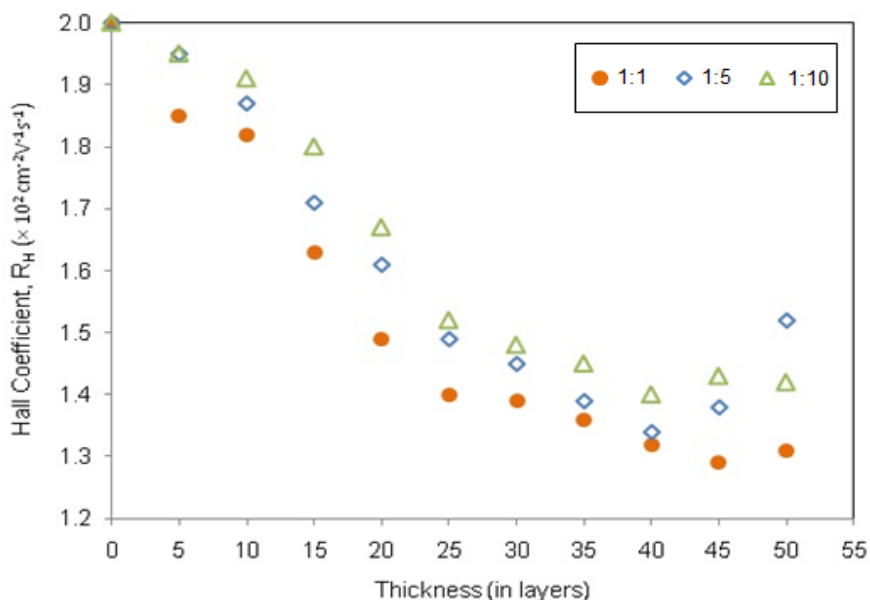


Figure 7: Hall coefficient variation against film thickness for varies CHLO samples

By referring to Figure 7, Hall coefficient is observed to decrease gradually as film thickness increases. The Hall coefficient range detected was between  $1.29 \times 10^2 \text{ cm}^2 \text{V}^{-1} \text{ s}^{-1}$  to  $2.0 \times 10^2 \text{ cm}^2 \text{V}^{-1} \text{ s}^{-1}$ . The commercial ITO (0 layer of film) of varies CHLO samples with  $2.0 \times 10^2 \text{ cm}^2 \text{V}^{-1} \text{ s}^{-1}$  was found as the highest Hall coefficient while the lowest Hall coefficient obtained for sample 1:1, 1:5, 1:10 were  $1.29 \times 10^2 \text{ cm}^2 \text{V}^{-1} \text{ s}^{-1}$  (at 45 layers),  $1.34 \times 10^2 \text{ cm}^2 \text{V}^{-1} \text{ s}^{-1}$  (at 40 layers) and  $1.40 \times 10^2 \text{ cm}^2 \text{V}^{-1} \text{ s}^{-1}$  (at 40 layers) respectively. The observation agrees with the theory experimental that the Hall coefficient decreases with the charge density,  $n$ . In thicker samples, the mobile charge carrier density increases as predicted. This is in agreement with the work reported by Pichard et al., (1981).

#### Carrier Concentration

The effect of film thickness on carrier concentration for PPy samples which can be seen in the Figure 8. It is apparent that the carrier concentration is increasing with increasing film thickness till 40 layers and then decreases for the higher thickness. This can be explained by the lack of Oxygen to compensate possible vacancies and so, to an enhancement on the bulk defects [11]. Furthermore, Oxygen vacancies induce free electrons as conduction carriers [12]. The carrier concentration was calculated from Equation (5).

The carrier concentration in the varied PPy samples was attested by their thickness, as shown in Figure 8. This relationship is found to be in good agreement reported by [13] and [14]. The lowest carrier concentration detected was  $3.125 \times 10^{16} \text{ cm}^{-2}$  for the commercial ITO (0 layer film). The highest carrier concentration detected for sample 1:1, 5:1 and 10:1 was  $4.830 \times 10^{16} \text{ cm}^{-2}$  (at 45 layers),  $5.00 \times 10^{16} \text{ cm}^{-2}$  (at 40

layers) and  $5.330 \times 10^{16} \text{ cm}^{-2}$  (at 40 layers) respectively. The carrier concentration increased as the amount of PPy in the blended samples increased. Therefore, sample 10:1 which contained 10:1 ratio of PPy:CHLO exhibited the highest carrier concentration for varies PPy samples. The carrier concentration detected was between  $3.125 \times 10^{16} \text{ cm}^{-2}$  to  $5.330 \times 10^{16} \text{ cm}^{-2}$ . The variation of carrier concentration for CHLO samples are plotted in Figure 9.

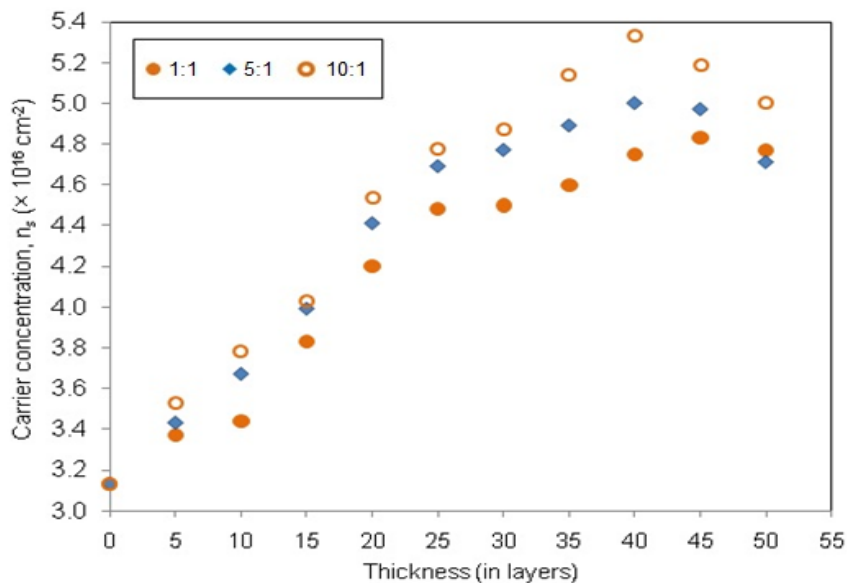


Figure 8: Carrier concentration of PPy samples film with respect to the thickness

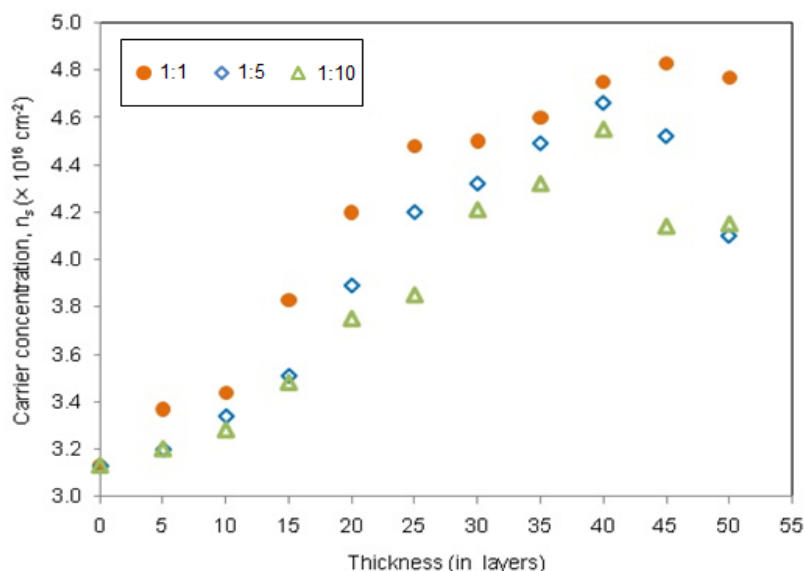


Figure 9: Carrier concentration of CHLO film with respect to the thickness

Figure 9 shows that the carrier concentration for varies CHLO sample increase with increase film thickness and then decrease a bit again for the higher thickness. The range of carrier concentration detected was between  $3.125 \times 10^{16} \text{ cm}^{-2}$  to  $4.83 \times 10^{16} \text{ cm}^{-2}$ . From these plots, it is apparent that the sample 1:1 (at 45 layers) exhibited the highest carrier concentration of varies CHLO samples with respect to the film thickness. This occurrence is due to the amount of CHLO in the blended samples which CHLO act as insulator. Thus, as amount of CHLO decreased,  $n_s$  increased. In addition, the carrier concentration obtained was  $10^{16} \text{ cm}^{-3}$  for P-type samples in this experiment is similar reported by [15]. The larger free carrier density is due to the low resistivity [16-17] and high conductivity of film [18].

### Hall Mobility

From measurement of Hall coefficient and resistivity, Hall mobility was calculated using Equation (6). Figure 10 present the Hall mobility graph as a function of film thickness for varies PPy samples.

By referring Figure 10, the Hall mobility is observed to increase from 0 layer to 5 layers of film thickness. This is due to the effect of thin film deposition (0 to 5 layers). However, the Hall mobility for samples 1:1, 5:1 and 10:1 decreased rapidly after 5 layers. Then, the Hall mobility is not constant over 25 layers of thickness. The lowest Hall mobility detected was  $33 \text{ cm}^2/\text{Vs}$  for the commercial ITO (0 layers of thickness). In contrast, the Hall mobility for sample 1:1 was  $44.60 \text{ cm}^2/\text{Vs}$ , for sample 5:10 was  $46 \text{ cm}^2/\text{Vs}$ , and for sample 10:1 was  $47 \text{ cm}^2/\text{Vs}$ . The highest point of Hall mobility was at 5 layers of film thickness. The range of Hall mobility observed was between  $33 \text{ cm}^2/\text{Vs}$  to  $47 \text{ cm}^2/\text{Vs}$ . Figure 11 present the Hall mobility variation with the film thickness for CHLO samples.

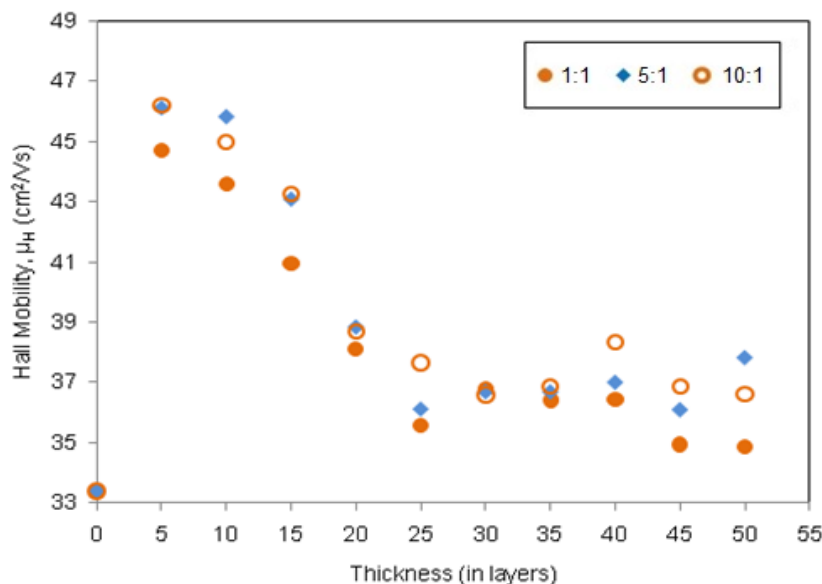


Figure 10: Hall mobility of PPy samples with respect to the thickness

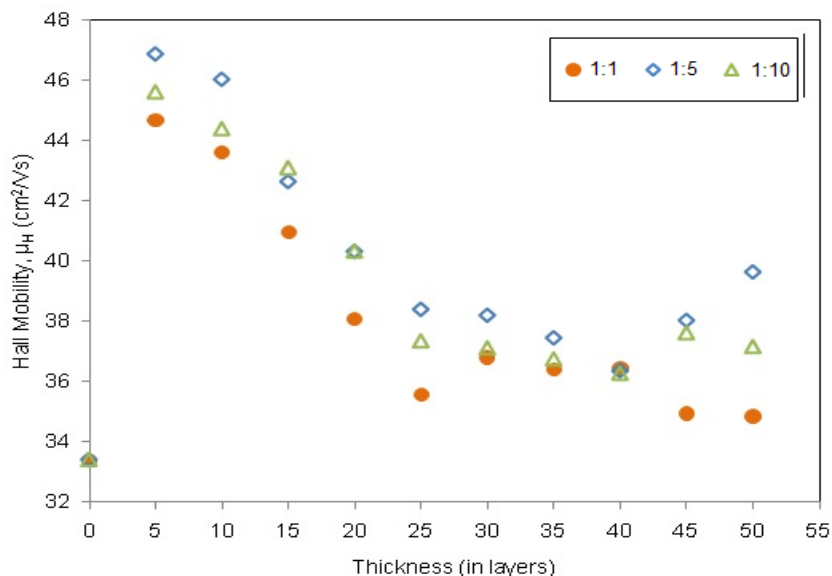


Figure 11: Hall mobility of CHLO samples with respect to the thickness

As PPy samples varies, in Figure 10, the Hall mobility for CHLO samples is dependent on the thickness. The results indicated that the Hall mobility decreased sharply until the thickness of 25 layers. Beyond 25 layers, the mobility appeared to be constant at about  $36.5 \text{ cm}^2/\text{Vs}$  on the average. The variation in the mobility is almost similar to the variation of Hall coefficient illustrated by Figure 7. This observation leads to the conclusion that the Hall coefficient plays a greater role on determining the mobility. Since the Hall coefficient is inversely proportional to the carrier concentration, it can be concluded further that the mobility changes are basically due to the changes in the carrier concentration.

#### *Type of Charge Carrier*

The charge carrier type can be determined by the polarity of the Hall voltage and Hall coefficient. If positive, the charge carriers are holes and the material is of the P-type. In this work, it was found that, the Hall voltage is positive for all samples. This finding indicates that the majority carriers are holes, according to the concept of semiconductors. These materials contained more holes than electrons, irrespective of the sign of the measured electrical properties [19]. In other words, since the Hall voltage is positive, the holes are major charge carriers for all samples.

### CONCLUSION

From the results, it can be concluded that the electrical carrier concentration increase with increase film thickness, and thus the electrical resistivity decrease with increase film thickness. The Hall mobility is reciprocal to the carrier concentration due to the lack of oxygen to compensate possible vacancies and so, to an enhancement on the bulk defects [11]. The Hall mobility does not change significantly with the film thickness as

obtained from this work. The thin films deposited at room temperature generally have amorphous structure, in the case of amorphous structure; it is known that Hall mobility does not change significantly. However, in the case of polycrystalline structure, Hall mobility changes significantly with grain size due to the electron scattering at the grain boundaries [20]. As the film thickness increase, the crystal grain size becomes bigger, which will lead to an obvious decrease of the density of the grain boundary and the carrier mobility. The thickest films were of the highest transparency in the visible region. The dependence of Hall mobility on the free carrier density reported. It is found that Hall mobility strongly depends on the carrier density.

### ACKNOWLEDGEMENT

The authors gratefully acknowledge to the Minister of Higher Education, Malaysia and Universiti Malaysia Terengganu for the financial supports, also co-authors for the invaluable idea and greet support. Vote number is 59156. Thanks are also due to the Physical Sciences laboratory for extensive usage of laboratory facilities.

### REFERENCES

- [1] M. Mahnaz Abdi, Anuar Kassim, H. N. M. Ekramul Mahmud, Wan Mahmood Mat Yunus, Zainal Abidin Talib, Amir R. Sadrolhosseini. *J Mater Sci* **44** (2009) 3682–3686
- [2] Anuar Kassim, Zulkarnain Zainal, Wan Mahmood Mat Yunus, Mohd Shahril Husin, Dzulkefly Kuang, Abdul Halim Abdullah and H. N. M. Ekramul Mahmud. *Solid State Science and Technology*, **12** (1) (2004) 29-35
- [3] R.E. Kirk and D.F. Othmer. (eds) “Encyclopedia of Chemical Technology”, 3rd Edn. John Wiley, Chichester 1979) 370—371
- [4] S. Hasiah, K. Ibrahim, H.B. Senin, and K.B.K. Halim. *Journal of Physical Science*, **19** (2) (2008) 77-92
- [5] J.W. Hammod and Chung-Chiun Liu. *Sensor and actuators B* **81** (2001) 25-31
- [6] M.K. Chong, K. Pita, S.T.H. Silalahi. Correlation between diffraction patterns and surface morphology to the model of oxygen diffusion into ITO films. *Journal of Materials Chemistry and Physics* **115** (2009) 154-157
- [7] S. Hasiah, E.A .Ghapur, N. Amalina, A.N. Faizah, Y. Nusaibah, K. Ibrahim. Proceeding of 9<sup>th</sup> International annual Symposium on Sustainability Science and Management held on 8<sup>th</sup> -11<sup>th</sup> May 2010 at Kuala Terengganu, Terengganu pp. 841-848.
- [8] S.Hasiah, K. Ibrahim, H.B. Senin, and K.B.K. Halim. Electrical Conductivity of Chlorophyll with Polythiophene Thin Film on Indium Tin Oxide as *P-N* Heterojunction Solar Cell. *Journal of Physical Science* **19** (2) (2008) 77–92
- [9] H. Salleh, “UMT Hall effect measurement software with corporation of Dr Salleh, LEIOS-Software and Nanorian technology,” unpublished.
- [10] 7600 series Hall system hardware references manual.

- [11] I. Baía, B. Fernandes, P. Nunes, M. Quintela, and R. Martins. Influence of the process parameters on structural and electrical properties of r.f. magnetron sputtering ITO films. *Thin Solid Films* **383** (1-2) (2001) 244-247
- [12] K.B. Sundaram and J. Blanchard, J. Deposition and annealing studies of indium tin oxide films. Proceedings IEEE Southeastcon '97. 'Engineering the New Century' held on 12<sup>th</sup> – 14<sup>th</sup> April 1997 at Blacksburg, USA 230– 232.
- [13] Hsin Her Yu, Shug-June Hwang, Ming-Chun Tseng, and Chien-Chang Tseng. *Optics Communications* **259** (1) (2006) 187-193.
- [14] Lei Hao, Xungang Diao, Huaizhe Xu, Baoxia Gu, Tianmin Wang. *Applied Surface Science* **254** (2008) 3504–3508
- [15] Haslinda Abdul Hamid. “Fabrication and Electrical Characteristics of RF Magnetron Sputtered P-type ZnO Films”, (Master Thesis, Universiti Sains Malaysia (USM) 2009.)
- [16] X.W. Sun, D.H. Kim, and H.S. Kwok. 1997. Ultra thin ITO films deposited on various substrates by pulsed laser deposition. MRS Proceeding in Boston, MA, USA, Dec 2-5, pp 485:267-72.
- [17] Shinji Takayama, Toshifumi Sugawara, Akira Tanaka, and Tokuji Himuro. *Journal of Vacuum Science Technology A* **21**(4) (2003) 1351-1354
- [18] S.A. Bashar. 1997. Study of Indium Tin Oxide (ITO) for Novel Optoelectronic Devices. PhD thesis. <http://www.betelco.com/sb/phd/acknowle.html>. Accessed on 7<sup>th</sup> July 2010.
- [19] C. Hilsum and A.C. Rose Innes. Semi conducting III-V compound. (Pergamon, Oxford, 1961) 120.
- [20] J.S. Kim, J.W. Bae, H.J. Kim, H.E. Lee, G.Y. Yeon, K.H. Oh. *Thin Solid Films* **377-378** (2000) 103-108